Magnetic excitations in the itinerant antiferromagnets Mn_3Si and Fe-doped Mn_3Si

S. Tomiyoshi, Y. Yamaguchi, and M. Ohashi
Research Institute for Iron, Steel and Other Metals, Tohoku University, Sendai 980, Japan

E. R. Cowley
Rutgers University, Camden College of Arts and Sciences, Camden, New Jersey 08102

G. Shirane
Brookhaven National Laboratory, Upton, New York 11973
(Received 16 March 1987)

Magnetic excitations in the itinerant antiferromagnets Mn_3Si and Fe-doped Mn_3Si have been measured at low temperatures by inelastic scattering of neutrons. Mn_3Si is an incommensurate antiferromagnetic with magnetic Bragg points of the form $(h,k,l)\pm(\delta,\delta,\delta)$ with $\delta=0.425$. Fe-doped Mn_3Si is a commensurate antiferromagnet with $\delta=\frac{1}{2}$. Its low-energy magnetic excitations have a linear dispersion relation with a slope of approximately 30 meV Å, but above 6 meV, the slope increases so that the "cone" of the dispersion relation becomes a "chimney." Well-defined excitations have been observed at energies up to $7.5k_BT_N$ (15 meV). In pure Mn_3Si, a similar dispersion cone exists around each satellite magnetic Bragg point with a slope of approximately 37 meV Å. The two dispersion cones from a pair of satellite points intersect at about 5 meV. Above this energy the intensity of the inelastic peaks changes drastically, indicating a strong interaction between the cones. For both phases, the damping is very large and increases almost linearly with energy.

I. INTRODUCTION

Itinerant-electron antiferromagnets are a most attractive class of systems for the investigation of the spin-wave excitations by means of neutron inelastic scattering, because the cross section of the excitations contains much information about their magnetic and electronic properties. The dispersion relation of spin waves in antiferromagnets is known to have a soundlike dispersion linear in q.[1] The most characteristic properties of the excitations in itinerant antiferromagnets which distinguish them from those in localized antiferromagnets are a steeply sloping dispersion relation persisting to very high energy, and large damping of the excitations.[1-5] The spin-wave velocity, i.e., the slope of the dispersion curve, has a large value, proportional to the electron velocity at the Fermi surface, as shown by Fedders and Martin for a nesting-type antiferromagnet.[1] The damping of the spin waves, which decay into electron-hole pairs, is expected to provide useful information about the band structure.[4-6] It has also been suggested that a resonancelike strong scattering may occur at the band-gap energy.[7]

The experiments done so far have been confined mainly to chromium,[3,8-10] chromium alloys,[11,12] and many kinds of γ-Mn alloys.[2,13,14] In chromium the magnetic excitations were found to emanate from incommensurate magnetic Bragg points with a very steep slope dispersion relation persisting to very high energies. A pair of inelastic peaks coalesce into a single peak centered at a Brillouin-zone boundary as the energy increases, and in addition to these another low-lying excitation was found between each pair of satellites.[3] Because of the steep slope of the dispersion relation and the large damping, the cone-shaped dispersion has not been resolved at any of the measured energies. In spite of many experiments, a complete picture of the magnetic excitations in chromium has not yet been established at present, because of the experimental difficulties of measuring at the high energies with enough resolution. Studies on γ-Mn alloys also met similar experimental difficulties, though the situation is somewhat easier than that in chromium. A good way to make further advances in understanding the magnetic excitations in itinerant antiferromagnets is to investigate experimentally easier samples, for which a low Néel temperature is essential since it represents the energy scale of the magnetic excitations involved. Mn_3Si is a very good candidate satisfying such a condition, since its Néel temperature is only 25.8 K,[15] an order of magnitude lower than that of chromium, and the spin structure is incommensurate.

Mn_3Si has the cubic crystal structure of DO_3 type (ordered Fe_3Al type) with the lattice constant $a=5.722$ Å.[16] The spin structure proposed is either a proper screw or a transversal sinusoidal structure. Which structure is correct has not been determined yet.[15] The magnetic satellite peaks with a propagation vector $Q=0.425a^*_{111}$, where a^*_{111} is a (111) reciprocal-lattice vector, appear near a Brillouin-zone boundary in pairs along a [111] direction. Figure 1(a) shows the crystal structure and Fig. 1(b) shows a $(01\bar{1})$ plane of the reciprocal lattice. There are two kinds of magnetic atoms in this structure. A Mn_I atom surrounded by eight nearest-neighbor Mn_{II} atoms has a magnetic moment of $1.7\mu_B$. Each Mn_{II} atom has four Mn_I and four Si atoms as its nearest neighbors and

has a smaller magnetic moment of $0.19\mu_B$. A Mn_I moment on the body center couples antiparallel to Mn_{II} moments on the body corner. The spin coupling is similar to that of chromium, except that the Mn_I and Mn_{II} atoms have different moments, and that every other bcc unit has a silicon atom at its center. In previous neutron-inelastic-scattering experiments,[17] it was found that the magnetic excitations in Mn_3Si emanate from each magnetic satellite point with fairly steep slope dispersion and the excitations have very broad linewidths. At higher energies a pair of peaks become a broad structureless peak. This behavior of the magnetic excitations resembles in many respects that in chromium, and is typical of the behavior found in itinerant antiferromagnets described above, so we can classify Mn_3Si as an itinerant antiferromagnet. The resolution of the early experiments was not high enough, so in the present experiment we try to measure with higher resolution and up to higher energies. We have also now made measurements on a sample of Mn_3Si doped with a small amount of iron. It has been found that the incommensurate phase becomes commensurate with this addition.[18] The spin-wave dispersion surface then consists of a single cone, and the analysis of the measured spectra is greatly simplified.

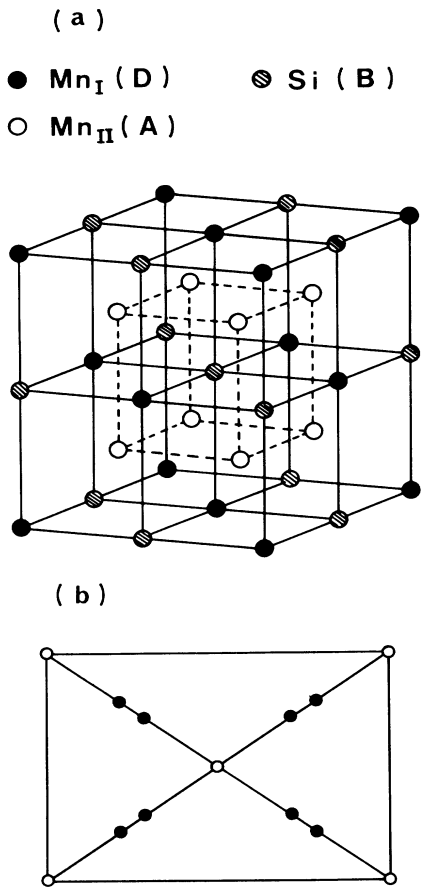

FIG. 1. (a) The structure of Mn_3Si. (b) $(01\bar{1})$ plane of the reciprocal lattice. The solid circles show the positions of magnetic Bragg points in the incommensurate phase.

II. EXPERIMENTAL DETAILS

The single crystal of Mn_3Si used in the present experiments was identical to that used in the previous experiment,[17] which was grown from the melt by the Czochralski method. The crystal shape is approximately cylindrical with its long axis 25° inclined from the $[01\bar{1}]$ direction. The size of the crystal is approximately 1 cm^3. The mosaic spread determined from the rocking curve of the (111) reflection is 45′. This crystal contains a small amount of a silicon-rich phase (probably Mn_5Si_3) as small particles, but we believe that this impurity does not have a serious effect on our experiments. We tried to grow pure single crystals by using various methods, but we could not succeed in growing crystals free from contamination of another phase.

A commensurate-phase crystal with the nominal formula of $Mn_{2.8}Fe_{0.2}Si$ was grown from the melt in an alumina crucible by the Bridgman method. It is a cylinder of volume 1 cm^3 and its long axis deviates approximately 40° from the $[01\bar{1}]$ direction. The mosaic spread is 54′. Each crystal was sealed in an aluminum can filled with He gas and mounted in a variable-temperature cryostat with the $[01\bar{1}]$ axis vertical to the scattering plane.

Neutron-inelastic-scattering experiments were carried out with a neutron triple-axis spectrometer at the Brookhaven High Flux Beam Reactor. Pyrolytic graphite reflecting from the (002) plane was used for both monochromator and analyzer. Most of the measurements were performed with a fixed out-going neutron energy of 14.7 meV and a pyrolitic graphite filter was inserted after the analyzer in the neutron beam path to remove higher-order contaminations. The incident beam was monitored by a fission counter placed after the monochromator.

III. ANALYSIS METHODS

The cross section for neutron inelastic scattering in a magnetic system is given by[19]

$$\frac{\partial^2\sigma}{\partial\Omega\, d\omega}=\frac{N}{h}(r_0\gamma)^2\frac{k_f}{k_i}\,|f(Q)|^2\tfrac{1}{4}(1+\tilde{K}_z^2)S(Q,\omega)\ , \tag{1}$$

where

$$S(Q,\omega)=\frac{\hbar}{\pi}[n(\omega)+1]\frac{1}{(q\mu_B)^2}\mathrm{Im}\chi(Q,\omega)\ , \tag{2}$$

and N is the number of scattering centers, namely spins, $f(Q)$ is the magnetic form factor, and $S(Q,\omega)$ is the scattering function which may be related to the imaginary part of the generalized susceptibility $\chi(Q,\omega)$. If the susceptibility is calculated theoretically, we can compare it with the observed data. However, in the present case there is no theoretical calculation on this material, so that it is necessary to assume a form for the spectral weight function, which is related to the imaginary part of the generalized susceptibility,

$$\mathrm{Im}\chi(q,\omega)=\omega\chi(Q)F(Q,\omega)\ , \tag{3}$$

where $\chi(Q)$ is the static wave-vector-dependent susceptibility and $F(Q,\omega)$ is the normalized spectral weight func-

tion describing the dynamics.

For the spectral weight function, a Lorentzian or a damped harmonic oscillator are most commonly used. In the present analysis we use a Lorentzian:

$$F(q,\omega)=(1/2\pi)\{\Gamma_q/[(\omega-\omega_q)^2+\Gamma_q^2 + \Gamma_q/[(\omega+\omega_q)^2+\Gamma_q^2]\}\ , \quad (4)$$

where the first and second terms correspond to creation and annihilation of a spin wave, respectively, ω_q is the resonant frequency representing the dispersion relation, and Γ_q is a damping factor, whose inverse is proportional to the lifetime of the spin wave. As many theories predict, we assume that dispersion is of the form

$$\omega_q^2=c^2q^2+D^2\ , \quad (5)$$

where c is the slope of the dispersion relation and D is its gap. If D is zero, this reduces to a linear dispersion relation. The damping is assumed to be linear in q,

$$\Gamma_q=\Gamma_0+\Gamma_1 q\ . \quad (6)$$

For the incommensurate phase we must consider two spectral weight functions corresponding to a pair of satellites,

$$F=P_1F(q_1,\omega)+P_2F(q_2,\omega)\ , \quad (7)$$

where P_1 and P_2 represent the intensities of the respective spin-wave excitations, which are proportional to the geometrical structure factors; q_1 and q_2 are the wave vectors of spin waves measured from their respective magnetic satellite points. We assume that the spectral weight functions F_1 and F_2 have identical slope of dispersion c and damping factor Γ.

The observed intensity is the convolution of the cross section and the resolution function $R(Q,\omega)$ which is represented by a four-dimensional ellipsoid.[20] The parameters included in the spectral weight functions are obtained by fitting the resolution-convoluted cross section with the observed intensity using a least-squares program.

IV. EXPERIMENTAL RESULTS

A. Fe-doped Mn_3Si

The magnetic phase diagram of the manganese-rich Mn_3Si and Fe_3Si system has not been well established, but it is known that the addition of a small amount of iron makes the incommensurate phase become commensurate and that accompanying this phase transformation the Néel-temperature variation is very smooth.[18] The crystal we used in the present experiments had the nominal formula $Mn_{2.8}Fe_{0.2}Si$ and was a magnetically single phase of the commensurate structure, whose unit cell is double that of the cubic chemical unit cell. Each pair of magnetic satellite points shown in Fig. 1(b) has coalesced into a single point at the Brillouin-zone boundary. The Néel temperature was determined from the temperature dependence of the $(\frac{1}{2},\frac{1}{2},\frac{1}{2})$ magnetic reflection to be 23 ± 0.5 K, which is a little lower than that of pure Mn_3Si.

We measured[21] magnetic excitations with constant-E scans mainly through $(\frac{1}{2},\frac{1}{2},\frac{1}{2})$ along the [111] direction [longitudinal scan (ξ,ξ,ξ)] and perpendicular to the [111] direction [transverse scan $(\xi, 0.75-\xi/2, 0.75-\xi/2)$]. Figures 2 and 3 show typical longitudinal and transverse scans through $(\frac{1}{2},\frac{1}{2},\frac{1}{2})$, except the data at 15 meV, which were measured through $(\frac{3}{2},\frac{3}{2},\frac{3}{2})$. All the excitation spectra are doublets corresponding to a single cone of a dispersion relation linear in q. Even at 1.5 meV the spectrum shows split peaks. As the energy increases, the width of the doublet increases gradually, and the excitations spread over a wider area of the Brillouin zone, though at high energies there is little change in the positions of the peak centers. There is no abrupt change in the character of the peaks. The solid lines are the result

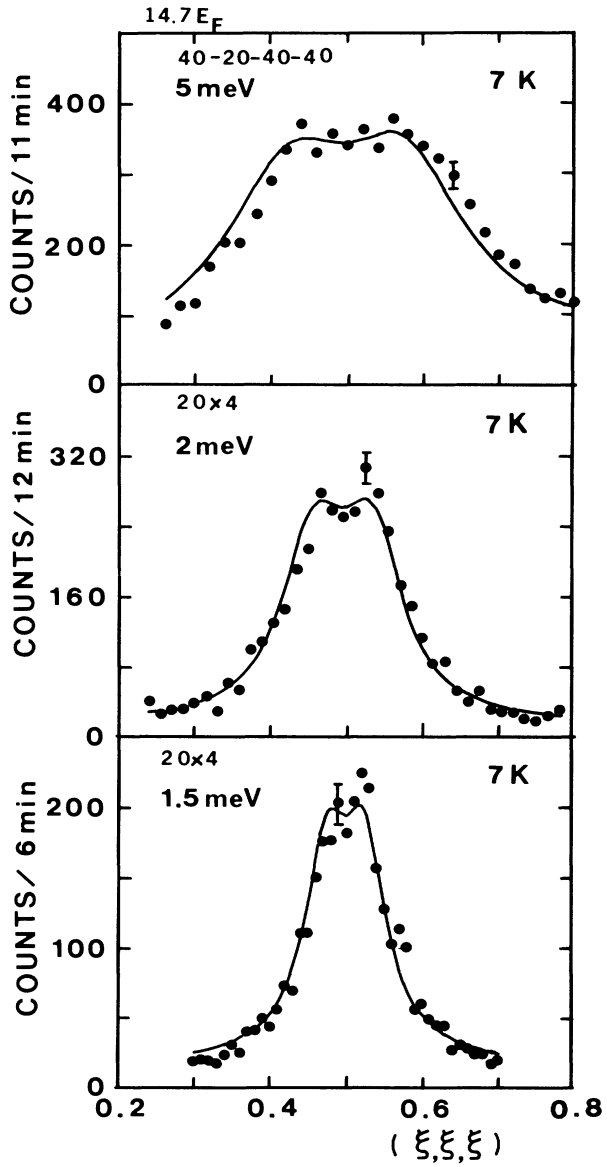

FIG. 2. Constant-energy scans along the [111] direction through $(\frac{1}{2},\frac{1}{2},\frac{1}{2})$ (longitudinal scans) in the Fe-doped sample of Mn_3Si. Lines are the results of a least-squares fit.

of the least-squares-fitting procedure described in Sec. III. The expression using a Lorentzian spectral function gives very good agreement with the experimental points at all energies. In this calculation we used the single Lorentzian form, Eq. (4), for the spectral function, with no gap in the dispersion relation, i.e., $D=0$.

Figure 4 shows the dispersion relations determined by the least-squares fitting for both the longitudinal and transverse scans. The slope of the dispersion is almost isotropic, which was confirmed below 5 meV by the measurements of both the longitudinal and transverse scans. The solid lines in the figure show a dispersion relation linear in q with a slope of 30 meV Å. At energy transfers below 8 meV, the data points follow these lines fairly well.

The most prominent feature of the dispersion curves is the increase of slope above 8 meV. The deviation of the observed points from the straight line is evident in the figure. This is the first experimental observation that a dispersion "cone" transforms into a "chimney." This "chimneylike" excitation persists up to the highest energy we measured, which was 15 meV, corresponding to $7.5k_BT_N$.

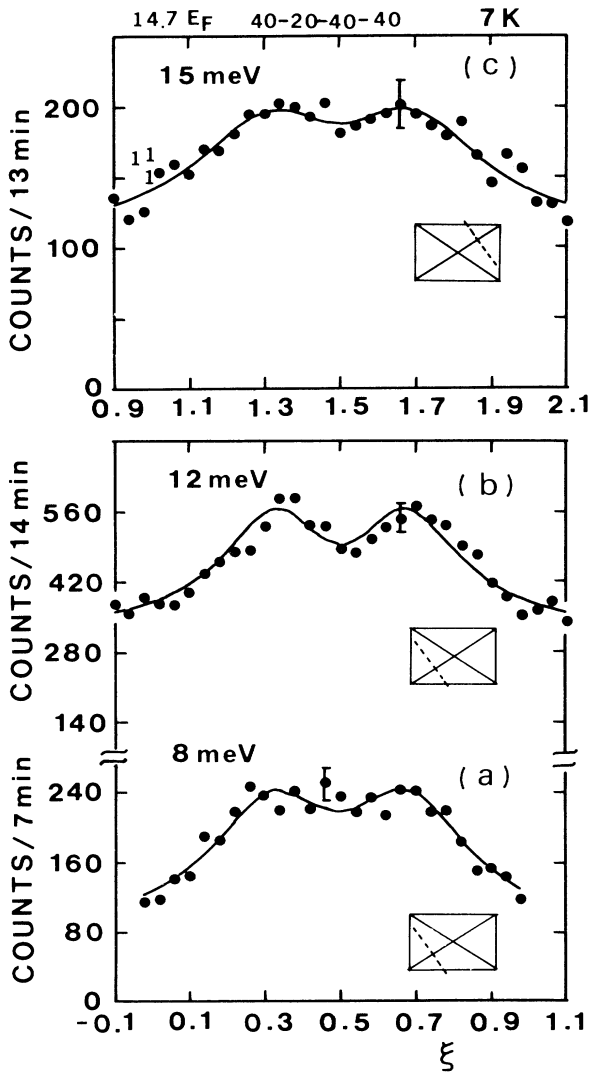

FIG. 3. Transverse constant-energy scans in the Fe-doped sample. (a) and (b) pass through the point $(\frac{1}{2},\frac{1}{2},\frac{1}{2})$, and (c) goes through $(\frac{3}{2},\frac{3}{2},\frac{3}{2})$.

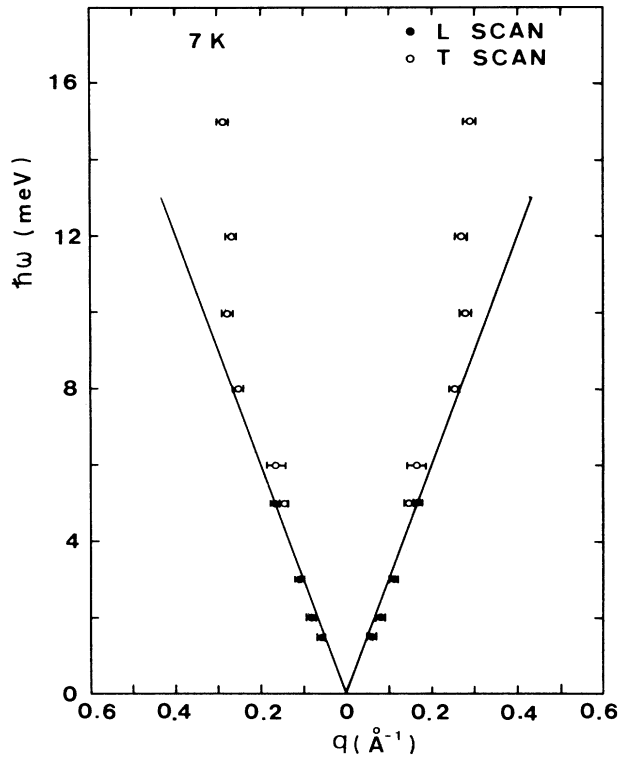

FIG. 4. Dispersion relation for the Fe-doped, commensurate, specimen. The straight lines correspond to a slope of 30 meV Å.

Figure 5 shows the total half-width, Γ_q, given by Eq. (6), as a function of energy. It is almost linear in energy and hence, at low energies, linear in q, as many theories have suggested. A linear dependence on energy would imply that above 8 meV the width increases rapidly with wave vector.

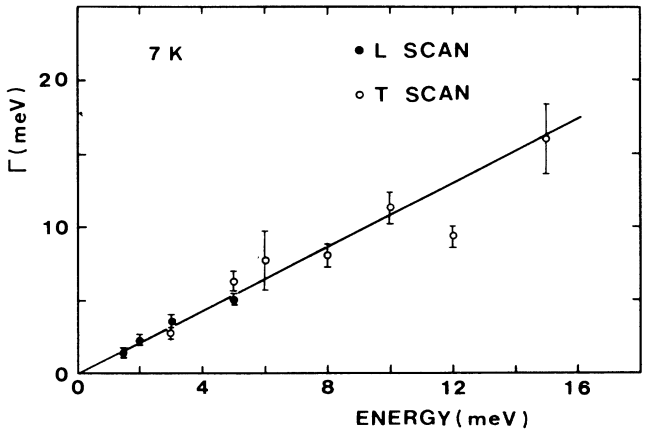

FIG. 5. Half-width Γ of the Lorentzian spectral function, in the commensurate specimen, as a function of energy. The line is a guide to the eye.

B. Mn_3Si

The inelastic scattering spectra measured through $(\frac{1}{2},\frac{1}{2},\frac{1}{2})$ along the [111] direction at low-energy transfers at 5.5 K are shown in Fig. 6. The spin-wave excitation peaks are single lines at 1 meV with fairly narrow linewidth whose widths are, however, somewhat wider than those of the elastic peaks inserted in Fig. 6(a). At 2 meV the width becomes wider and at 3 meV each single peak splits into a doublet. In the commensurate phase the peak was already split at 1.5 meV. This suggests that the slope of dispersion curve is slightly greater in the incommensurate phase. In our previous experiment[17] we could not observe well-split peaks above 2 meV, probably due to poor resolution and poor counting statistics. The cone was also confirmed by measuring along the $[1\,\bar{1}\,\bar{1}]$ direction through the satellite point (0.575, 0.575, 0.575). The peak is a doublet, in agreement with the longitudinal scan in Fig. 6(c). The solid lines in the figures are calculated values assuming that the cross section can be written in terms of two Lorentzian spectral weight functions and that the dispersion relation is linear in q, as mentioned in Sec. III (i.e., $D=0$). The good agreement between observed and calculated values shows that the cross section assumed is satisfactory in the present case up to an energy transfer of 3 meV.

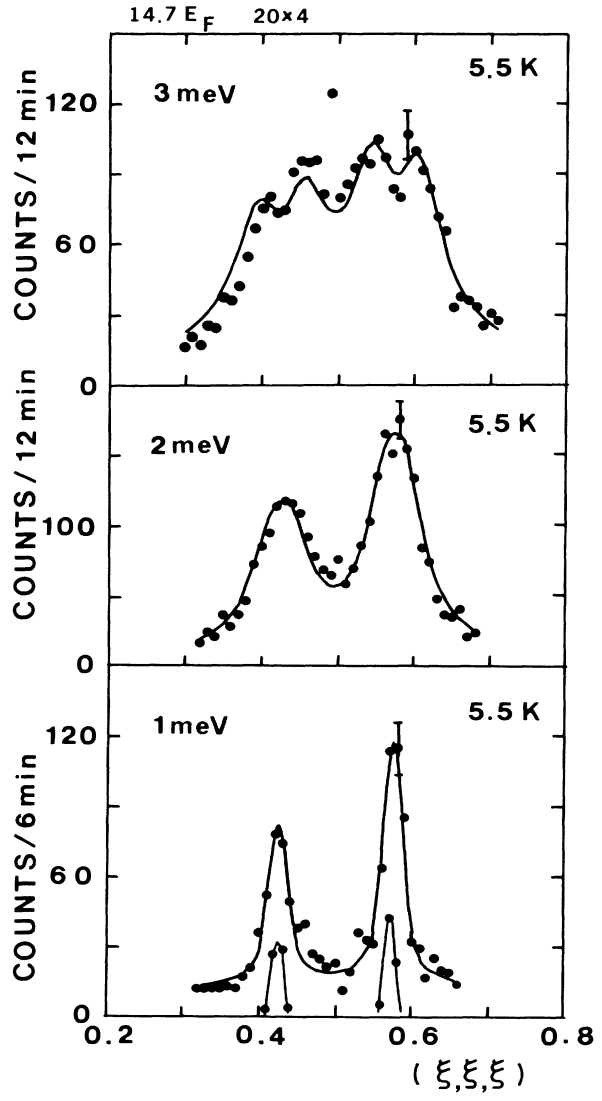

FIG. 6. Constant-energy scans along the [111] direction through $(\frac{1}{2},\frac{1}{2},\frac{1}{2})$ (longitudinal scans) in the pure, incommensurate specimen of Mn_3Si. Lines are the results of a least-squares fit. The elastic peaks are superimposed on (a).

The cones associated with a pair of magnetic satellite points overlap at 5 meV, as shown in Fig. 7. Above that the central peak loses its intensity. It is still observable above 10 meV, but its intensity is very weak. Above 6 meV we measured along the $[1\bar{1}\,\bar{1}]$ direction through the satellites around $(\frac{3}{2},\frac{1}{2},\frac{1}{2})$. Figure 8(b) shows such a scan. It should be noted that, since the structure factors $|P|^2$ for satellites belonging to 111, 000, and 200 indices are proportional to $\mu_{\rm I}^2$, $(\mu_{\rm I}-2\mu_{\rm II})^2$, and $(\mu_{\rm I}+2\mu_{\rm II})^2$, respectively, where $\mu_{\rm I}$ and $\mu_{\rm II}$ are the magnetic moments of $Mn_{\rm I}$ and $Mn_{\rm II}$ atoms, the intensity ratios of the satellites (δ,δ,δ) and $(1-\delta,\,1-\delta,\,1-\delta)$ are not the same as those of $(1+\delta,\,1-\delta,\,1-\delta)$ and $(2-\delta,\,\delta,\,\delta)$, but their ratios are not much different. The excitation spectra at 6 and 10 meV shown in Fig. 8 show similar patterns. At 10 meV the central peak is very weak, but it remains observable

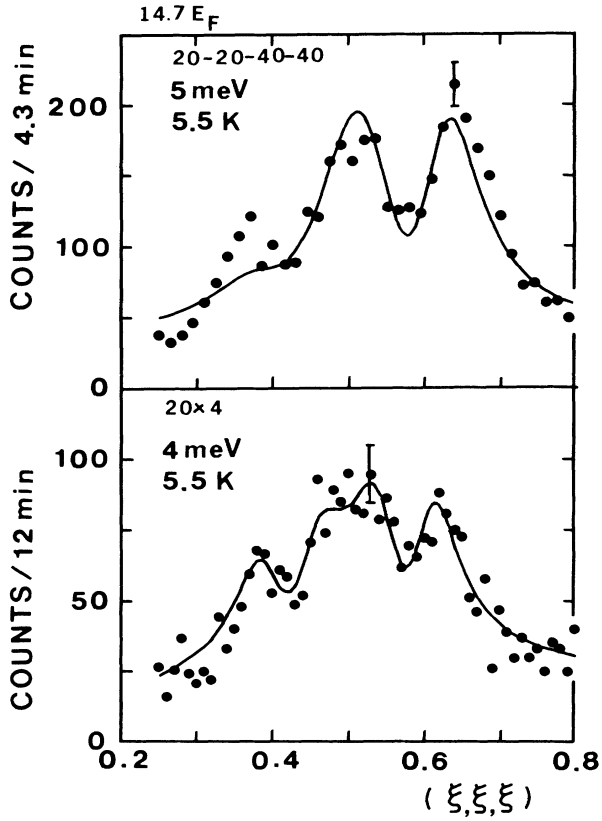

FIG. 7. Longitudinal constant-energy scans along the [111] direction through $(\frac{1}{2},\frac{1}{2},\frac{1}{2})$ in the pure Mn_3Si specimen. The fit worsens at 5 meV.

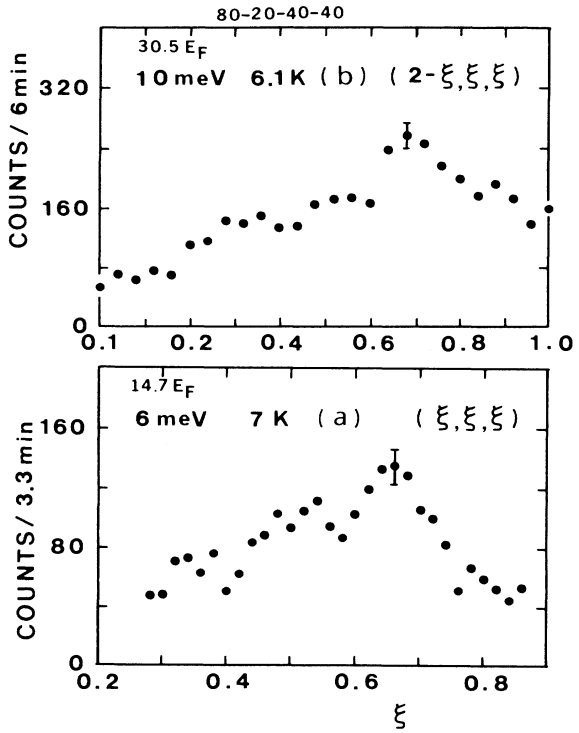

FIG. 8. Longitudinal constant-energy scans in the pure Mn_3Si specimen. (a) is along the [111] direction through $(\frac{1}{2},\frac{1}{2},\frac{1}{2})$; (b) is along the $[1\,\bar{1}\,\bar{1}]$ direction through $(\frac{3}{2},\frac{1}{2},\frac{1}{2})$.

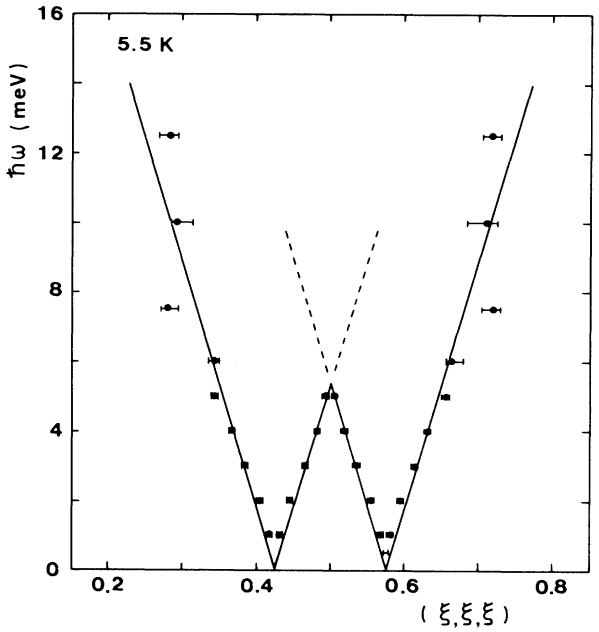

FIG. 9. Dispersion relation in the longitudinal direction for the incommensurate specimen of Mn_3Si, at 5.5 K. The straight lines correspond to a slope of 37 meV Å.

even at 12.5 meV, which is the highest energy we measured in this case.

The solid lines are fitted as for the other spectra; however, as shown in Fig. 7(b), in this case the line does not reproduce the observed data above 5 meV because of the decrease in intensity of the central peaks at the crossing of two dispersion cones. The assumption that the cross sections for a pair of satellites are a simple superposition of two Lorentzian spectra weight functions is apparently no longer valid above 5 meV. Therefore, above the crossing we determined the dispersion by fitting the observed data with four Lorentzians which have a common width and a common peak position from the respective satellite points, but with no restrictions on their respective peak heights. In this calculation the resolution function has not been included since the natural width is so large. Figure 9 shows the dispersion relations thus obtained. The experimentally determined points generally agree with the linear dispersion law of $\hbar\omega = cq$, with $c = 37$ meV Å, shown as straight lines in the figure.

At lower energies the experimental points seem to deviate a little toward the higher-slope side from the straight lines. Accurate determination of the slope of the dispersion curve is difficult when the observed peak is single, as was found below 2 meV in the present case. However, a lower limit of the slope is determined with fairly good accuracy by comparing the line profile with the observed data. The deviation of the points from the straight line below 2 meV is apparent, which suggests that the spin-wave excitations emanate initially with higher slope. If there is a gap in the dispersion relation as found in γ-Mn alloys,[13,14] the observed initial slope would have a larger value near the gap energy than that estimated from the straight part of the dispersion. In order to confirm this point, we performed a constant-Q scan at $Q = (0.577, 0.577, 0.577)$ with Be-filtered incident neutrons of energy 5 meV. Figure 10 shows the constant-Q data. The abrupt increase of counts below 0.2 meV is due to elastic scattering. The decrease in counts above 0.2 meV is gradual and there is no apparent indication of the presence of a gap. These data indicate that there is no gap above 0.2 meV. If the gap energy is lower than 0.2 meV, its effects on the linear-dispersion curve above 0.5 meV will be negligibly small. Thus we can conclude that the deviation of the dispersion curve from the straight line is caused by a large initial slope.

The inner two branches cross at 5 meV, and below that energy we observed well-defined branches. However, the excitations above that energy are obscure. We can still observe the central peak up to 12.5 meV, but its line shape is not clear and its intensity is very weak, so that we are not confident whether the excitations continue like the dotted lines extrapolated from the lower part of the branches as shown in Fig. 9. When two straight dispersion curves cross, the branches are expected to separate into a lower and an upper branch, and a gap develops between them. In Mn_3Si the modification of the dispersion curve just below the crossing point is very small, which indicates that the gap is very small if it exists. When the two cones touch not only the intersecting two branches—but also the left-hand-side branch—change in intensity. Figure 11 shows the intensity ratio of the left-hand-side branch 1 to the right-hand-side branch 4 as a function of

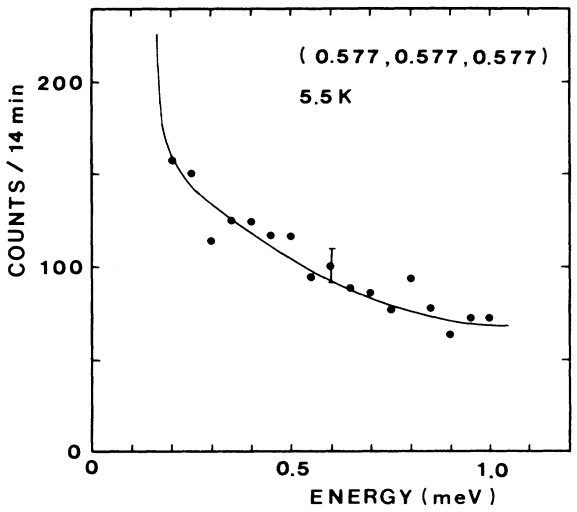

FIG. 10. Constant-Q scan through the magnetic Bragg point (0.577, 0.577, 0.577) of the incommensurate specimen. The solid line is a guide to the eye. At energies below 0.2 meV the points are out of range.

energy. This ratio decreases beyond 4 meV, where the crossing of the inner two branches begins. It is very strange that the outer two branches which do not contribute directly to the crossing are greatly affected by the crossing of the other side of the cones. This seems to show that there is strong interference between the two dispersion cones. Above 8 meV in the commensurate phase, the dispersion "cone" becomes a "chimney." In the incommensurate phase we were not able to obtain such a clear indication because of the complication of the overlapping of the two cones.

We made similar measurements of the magnetic excitations at a higher temperature of 15 K ($0.58T_N$) up to an energy transfer of 6 meV. The excitation spectra were essentially similar to those obtained at 5.5 K except for a small increase of the linewidths, though compared to the spectra at 5.5 K the fine structure is less distinct. Figure 12 shows the dispersion relation obtained at 15 K. The solid lines in the figure show a dispersion law linear in q with a coefficient $c = 37$ meV Å being the same one as displayed in Fig. 9 at 5.5 K. The data points generally follow this dispersion curve. This result suggests that the change of the dispersion relation is very small when temperature is increased up to $0.6T_N$. However, Fig. 13 shows that the damping has increased somewhat at 15 K.

V. DISCUSSION

In the commensurate, iron-doped sample we were able to study the excitations around an isolated magnetic Bragg point, up to the relatively high energy of $7.5k_BT_N$ (15 meV). Below 8 meV the dispersion surface is a cone with a slope of approximately 30 meV Å, but above this energy the slope increases considerably. We believe this is the first observation of such behavior. Hennion *et al.*[2] observed, in a manganese-rich Mn-Ni alloy, a linear dispersion relation almost to the Brillouin-zone boundary, but

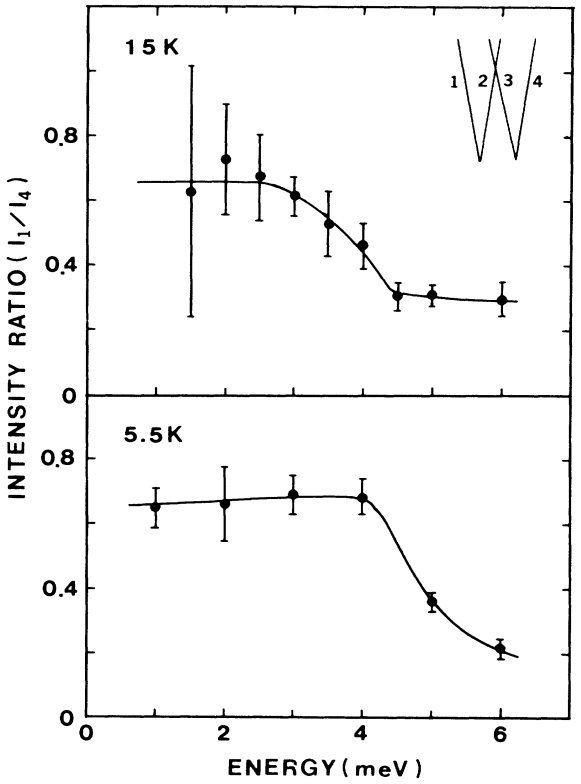

FIG. 11. Ratio of intensities of the two outer peaks as a function of energy, at 5.5 and 15 K.

in units of k_BT_N their measurements correspond only to the sloping part of our results. While the dispersion curve appears to be continuous, we note that above 8 meV the line shapes are extremely broad, so that there may be a change in character of the excitations at this point. In ferromagnetic Mn-Si, Ishikawa *et al.* observed two types of

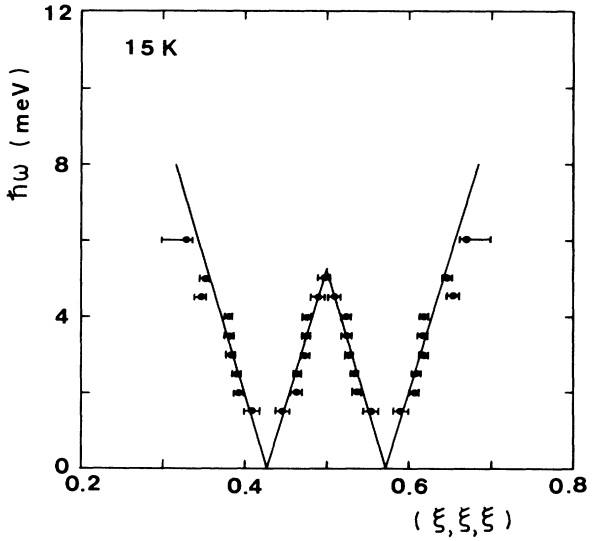

FIG. 12. Dispersion relation in the longitudinal direction for the incommensurate specimen of Mn_3Si, at 15 K. The straight lines correspond to a slope of 37 meV Å.

excitation[22] which they interpreted as spin waves with energies up to 3 meV, and Stoner excitations extended mover most of the Brillouin zone at higher energies, up to 18 meV ($7.7k_BT_c$). In the present case we cannot observe such a clear distinction. Also, the upward curve to the dispersion relation is different in our case.

The value of the slope, and of the Γ values shown in Fig. 5, are somewhat tentative in that they may depend on the assumed Lorentzian form for the spectral function. An earlier analysis[21] using a damped-harmonic-oscillator form gave rather different values. The present analysis is more satisfactory since the parameter values remain consistent from one energy to another.

The most obvious difference between the dispersion curves in the incommensurate and commensurate phases is that in the incommensurate phase there are two cone-shaped surfaces which intersect at 5 meV. There is some indication that the slope of the cones is greater in the incommensurate material (37 meV Å as compared with 30 meV Å). Since the slope is believed to be connected with the Fermi velocity, it is reasonable that it will be modified if the Mn_3Si is doped with iron. It is also possible that at very low energies the excitations in the incommensurate sample have an even greater slope. We were not able to follow the dispersion curves up to as high an energy in the incommensurate phase as the commensurate, and thus we are not sure that a similar narrowing into a "chimney" occurs.

In the region where the cones overlap, we see no evidence for a decreased energy at the crossing point, caused by hybridization of the cones, as predicted by Liu.[23] Nor can we distinguish four separate peaks in constant-energy scans above the crossing point. Rather there is a central peak, which persists to the highest energies, and two outer peaks. The ratio of intensities of these outer peaks changes quite strongly around the crossing energy.

The obvious material to make a comparison with is chromium. In chromium, because of the much higher Néel temperature, the whole energy scale is less well suited to neutron experiments. The cones around each of the incommensurate points are not individually resolved. Two of the most interesting features of the results[3,8] are that an additional excitation is found, at the commensurate position, with an energy of 4 meV, and that there appears to be an inward shift to the scattering at higher energies—the scattering gradually changes into a single peak over the commensurate position. As far as the first result is concerned, an energy of 4 meV scaled by the ratio of the Néel temperatures is equivalent to 0.3 meV in Mn_3Si. This is already difficult to distinguish from the elastic scattering. The second feature, the inward drift, may be related to the strong changes in intensity we measure in the outer lines. If both outer lines grew weak relative to the center, the effect seen in chromium might be reproduced.

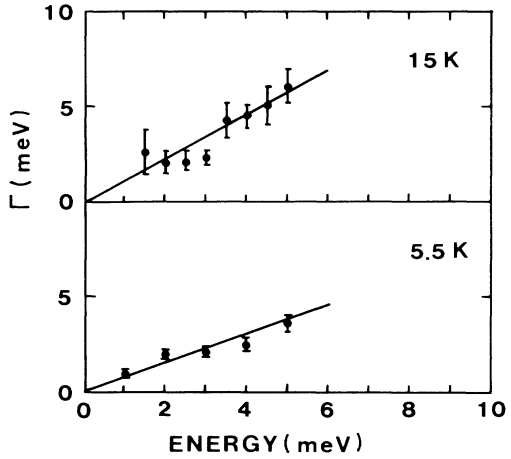

FIG. 13. Half-width Γ of the Lorentzian spectral function, in the incommensurate specimen, at 5.5 and 15 K, as functions of energy. The straight lines are guides to the eye.

Sokoloff[7] suggested that there may be a strong collective excitation at the band-gap energy for a gap-type itinerant antiferromagnet, and Ziebeck and Booth[8] showed that for chromium the integrated intensities of the constant-E peaks displayed a knee at 27 meV, which they associated with this excitation. In the present experiments we find that in the incommensurate phase the integrated intensities show a maximum at 2–3 meV. However, the exact value depends on the resolution, and the subtraction of the background is also difficult. We cannot therefore clearly confirm the presence of this resonance.

The main advantage of the present choice of material is the low value of the Néel temperature (25.8 K in the pure material). This results in the whole energy scale of the excitations being well suited for neutron spectroscopy, allowing many more details of the dispersion relations to be studied than previously.

ACKNOWLEDGMENTS

This work was carried out under the U.S.-Japan Cooperative Neutron Scattering Program. Work at Brookhaven National Laboratory was supported by the Division of Materials Sciences, U.S. Department of Energy, under Contract No. DE-AC02-76CH00016.

[1]P. A. Fedders and P. C. Martin, Phys. Rev. **143**, 245 (1966).
[2]B. Hennion, M. T. Hutchings, R. D. Lowde, M. W. Stringfellow, and D. Tocchetti, in *Proceedings of the Conference on Neutron Scattering*, edited by R. M. Moon (National Technical Information Service, Springfield, Virginia, 1976), pp. 825–831.
[3]C. R. Fincher, Jr., G. Shirane, and S. A. Werner, Phys. Rev. B **24**, 1312 (1981); Phys. Rev. Lett. **43**, 1441 (1979).
[4]M. J. Gillan, J. Phys. F **3**, 1874 (1973).
[5]A. F. Cade and W. Young, Adv. Phys. **26**, 393 (1977).
[6]S. H. Liu, Phys. Rev. B **2**, 2664 (1970).
[7]J. B. Sokoloff, Phys. Rev. **185**, 770 (1969); **185**, 783 (1969).

[8]K. R. A. Ziebeck and J. G. Booth, J. Phys. F. **9**, 2423 (1979).
[9]S. K. Burke, W. G. Stirling, R. A. Ziebeck, and J. G. Booth, Phys. Rev. Lett. **51**, 494 (1983).
[10]B. H. Grier, G. Shirane, and S. A. Werner, Phys. Rev. B **31**, 2892 (1985).
[11]J. Als-Nielson and O. W. Dietrich, Phys. Rev. Lett. **22**, 290 (1969).
[12]S. K. Sinha, S. H. Liu, L. D. Muhlestein, and N. Wakabayashi, Phys. Rev. **23**, 311 (1969).
[13]K. Tajima, Y. Ishikawa, Y. Endoh, and Y. Noda, J. Phys. Soc. Jpn. **41**, 1195 (1976).
[14]M. C. K. Wiltshire, M. M. Elcombe, and C. J. Howard, J. Phys. F **15**, 1595 (1985).
[15]S. Tomiyoshi and H. Watanabe, J. Phys. Soc. Jpn. **39**, 295 (1975).
[16]B. Aronson, Acta Chem. Scand. **14**, 1414 (1960).
[17]S. Tomiyoshi, S. Funahashi, and Y. Yamaguchi, Physica **120B**, 143 (1983).
[18]M. Ohashi and S. Tomiyoshi (unpublished).
[19]W. Marshall and S. W. Lovesey, *Theory of Thermal Neutron Scattering* (Oxford University Press, London, 1971).
[20]M. J. Cooper and R. Nathans, Acta Crystallogr. **28**, 357 (1967).
[21]A preliminary account of this part of the experiments has been reported in E. R. Cowley, S. Tomiyoshi, Y. Yamaguchi, M. Ohashi, and S. Shirane, Proceedings of the 1986 Conference on Magnetism and Magnetic Materials [J. Appl. Phys. **61**, 3403 (1987)].
[22]Y. Ishikawa, G. Shirane, and J. A. Tarvin, Phys. Rev. B **16**, 4956 (1977).
[23]S. H. Liu, J. Magn. Magn. Mater. **22**, 93 (1983).